Remote Sensing of Environment 153 (2014) 40–49

Contents lists available at ScienceDirect

Remote Sensing of Environment

journal homepage: www.elsevier.com/locate/rse

Monitoring dry vegetation masses in semi-arid areas with MODIS SWIR bands

Damien Christophe Jacques [a,*], Laurent Kergoat [b], Pierre Hiernaux [b], Eric Mougin [b], Pierre Defourny [a]

[a] Earth and Life Institute, Université Catholique de Louvain, Belgium
[b] Geosciences Environnement Toulouse (GET, CNRS/UPS/IRD/CNES), Toulouse, France

ARTICLE INFO

Article history:
Received 14 March 2014
Received in revised form 26 July 2014
Accepted 28 July 2014
Available online 17 August 2014

Keywords:
Dry vegetation
Mass
MODIS
Semi-arid areas
Sahel
Monitoring
Rangeland

ABSTRACT

Monitoring the mass of herbaceous vegetation during the dry season in semi-arid areas is important for a number of domains in ecology, agronomy, or economy and remote sensing offers relevant spatial coverage and frequency to that end. Existing remote sensing studies dedicated to dry herbaceous vegetation detection are mainly motivated by the assessment of soil tillage intensity and soil residue management, risk of soil erosion, and risk of wildfire linked to the mass of dead fuel. Few studies so far have dealt with monitoring of straw and litter degradation during the dry season over large areas while they are important fodder for livestock sustainability. MODIS band combinations (NBAR collection 5) were tested against a set of field measurements carried out over 20 rangeland sites from 2004 to 2011 in the Sahel. The best empirical linear models were obtained for indices using MODIS bands in the shortwave infrared domain (Band 6 centered at 1.6 μm, Band 7 centered at 2.1 μm), in particular with the Soil Tillage Index (STI). STI explained 66% of the variance of dry masses ($Mass = 3158(STI - 1.05)$, $r^2 = 0.66$, RMSE = 280 kg DM/ha, n = 232) for dry and intermediate season data. A regression is also proposed for year-round data ($Mass = 3371(STI - 1.06)$, $r^2 = 0.67$, RMSE = 352 kg DM/ha, n = 536). The strong inter-site and inter-annual variabilitieswere well captured and the decay rate was found consistent with grazing intensity and fire occurrence. The results imply that the STI can be applied to monitor the mass of dry tissues in the Sahel and potentially in many semi-arid areas.

1. Introduction

Semi-arid areas are characterized by a long dry season, during which annual plants die and perennial herbaceous plants often suffer drought by letting above-ground tissues dry while the below-ground parts survive. During the dry season, many physical and ecological processes, as well as some economical activities, interact with the amount and distribution of these above-ground dry tissues. Livestock sustainability for instance, depends on available fodder, which mostly consists of dry herbaceous plants. This resource varies throughout the year and from year to year. In the Sahel, for example, the extreme drought of 1984 resulted in very low plant production and extremely low dry-season fodder, which had severe impact on livestock survival and thus on pastoral population. In this context, assessing dry-season forage resources is a major concern and remote sensing offers relevant spatial coverage and frequency to that end. Frequent and accurate assessment of dry tissues is also very useful to studies of soil erosion, fire emissions biogeochemical cycles and surface energy budget (Barbosa, Stroppiana, Grégoire, & Cardoso Pereira, 1999; Samain et al., 2008; Shinoda, Gillies, Mikami, & Shao, 2011) in West Africa, but more generally in most arid and semi-arid areas worldwide (e.g. (Dregne, 2011)).

During the last decade, a number of remote sensing studies have addressed the detection of dry vegetation, pursuing different objectives: derivation of soil tillage intensity, soil conservation (Daughtry & Hunt, 2008; Daughtry, Hunt, Doraiswamy, & McMurtrey, 2005; Daughtry et al., 2006), evaluation of soil erosion risk and runoff (Arsenault & Bonn, 2005; Bannari, Chevrier, Staenz, & McNairn, 2007; Bergeron, 2000; Biard & Baret, 1997), evaluation of the risk of wildfire in relation to dead fuel proportion (Cao, Chen, Matsushita, & Imura, 2010; Elmore, Asner, & Hughes, 2005; Roberts et al., 2003) and improvement in land cover mapping (Guerschman et al., 2009; Peña-Barragán, Ngugi, Plant, & Six, 2011). The spectral signature of dry canopies and its application in the field has been extensively discussed by Nagler, Daughtry, & Goward(2000); Nagler, Inoue, Glenn, Russ, & Daughtry(2003) and Daughtry, Gallo, Goward, Prince, & Kustas(1992) among others. Few studies focused on dry season forage estimation, in terms of mass for instance (Ren & Zhou, 2012), and even fewer studies have tested monitoring methods efficient at large scale, since field or airborne spectroscopy or high resolution data from Landsat (Marsett et al., 2006; Serbin, Hunt, Daughtry, McCarty, & Doraiswamy, 2009; Zheng, Campbell, & de Beurs,

* Corresponding author.
E-mail address: damien.jacques@uclouvain.be (D.C. Jacques).

http://dx.doi.org/10.1016/j.rse.2014.07.027
0034-4257/

2012) or Hyperion (Daughtry et al., 2006; Guerschman et al., 2009; Monty, Daughtry, & Crawford, 2008; Roberts et al., 2003) were used in most cases.

Different factors potentially impair the detection of dry vegetation masses.

1. The similarity between soil and dry vegetation spectral signatures (Gausman, Wiegand, Leamer, Rodriguez, & Noriega, 1975) as well as the diversity of the soil spectral signature, which depends on factors such as mineralogy, structure, texture, and moisture (Aase & Tanaka, 1991; Baret, Jacquemoud, & Hanocq, 1993; Serbin, Daughtry, Hunt, Brown, & McCarty, 2009).
2. The structure of the vegetation, depending on the species and on the canopy architecture (standing grasses or litter for instance) (Daughtry, Serbin, Reeves, Doraiswamy, & Hunt, 2010; Kokaly & Clark, 1999; Wanjura & Bilbro, 1986).
3. The biochemical composition and state (C/N ratio, water content, tissue aging, photosynthesis activity) (Daughtry & Hunt, 2008).
4. The impact of wild or controlled fires on spectral properties (Lewis et al., 2010).

Ideally, a dry-season forage index allowing the retrieval of the mass of plant tissues should cope with all these effects. Furthermore, it should be derived on a week-to-week basis to capture forage dynamics along the season.

The objective of the present study is to investigate the relationship that exists between several reflectances and indices and masses of standing straws and litter using MODIS data from TERRA and AQUA satellites. For that purpose, radiometric indices are evaluated, through empirical linear models, against a set of field measurements collected over 8 years for a network of sites in the Sahel. Furthermore, the sensitivity of mass retrieval to the structure of the vegetation (proportion of standing straws and litter), the season and thus the water content, the presence of photosynthetic vegetation, the soil background, and the burn scars are analyzed to determine the robustness of the method.

2. Background

2.1. Spectral characteristics of dry vegetation

The spectral regions mostly used to assess crop residue cover, litter or more generally dry or non-photosynthetic vegetation on the ground are the visible (VIS, 0.4–0.7 μm), near infrared (NIR, 0.7–1.2 Im) and shortwave infra-red (SWIR, 1.2–2.5 μm) domains. The use of the VIS–NIR domain is debated because of difficulties to distinguish dry vegetation from the underlying ground. Indeed, in this spectral region, soil and dry vegetation both display a wide range of spectral signatures, with soil reflectance being lower or higher than the dry vegetation is (Aase & Tanaka, 1991; Nagler et al., 2000; Nagler et al., 2003). The SWIR domain contains absorption features of dry vegetation at 1.7, 2.1 and 2.35 μm (Fig. 1). Elvidge(1990) has observed absorption features at 2.1 and 2.3 μm using Airborne Visible Infrared Imaging Spectrometer (AVIRIS) data over dry shrubs. Absorption in the SWIR has been associated with structural compounds as cellulose, hemicellulose and lignin since non-structural compounds as sugars and starches are already degraded by microorganisms in dry material (Elvidge, 1990; Roberts, Smith, & Adams, 1993; Roberts et al., 1990). As leaf water content increases, these absorption features are impacted by spectral properties of water (Kokaly, Asner, Ollinger, Martin, & Wessman, 2009; Kokaly & Clark, 1999; Serbin, Daughtry, Hunt, Brown, & McCarty, 2009).

2.2. Dry vegetation indices

The signature of dry matter compounds in the SWIR domain has fostered the emergence of various indices, most often for discriminating dry vegetation from green vegetation and soil background. Table 1 presents the formula of the indices described hereafter.

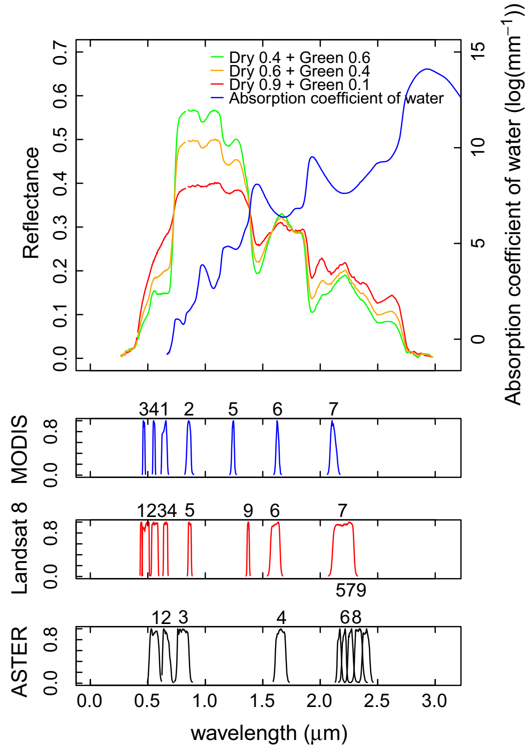

Fig. 1. Spectral signatures of areal mixtures of dry long grass collected early August and lawn grass picked on June, from the USGS digital spectral library (Clark et al., 2007) and the absorption coefficient of water (data from (Bertie & Lan, 1996)). Relative spectral responses of bands from MODIS, Landsat 8 and ASTER are also represented. Note that the MODIS band 7 (2.061–2.167 μm) falls into the absorption feature characteristic of dry vegetation at 2.1 μm. Other absorption features at 1.7 and 2.35 μm can be also observed on spectral signature of scene dominated by dry vegetation (red curve).

Based on the spectral absorption feature at 2.1 μm, the Cellulose Absorption Index (CAI) was defined by Daughtry(2001). This index has been demonstrated many times to be suitable to detect dry vegetation

Table 1
Dry vegetation indices from literature. ρ_x is the reflectance of the wavelength in the band x. TM, A, M correspond to Landsat TM, ASTER, MODIS bands respectively. a and b are the slope and the intercept of the soil line in the corresponding spectral band domain. $L = 1 - 2a$. $NDSVI$. $(\rho_{TM5} - a\rho_{TM5})$. δ is the angle between the soil and the residue lines. ζ is the angle between the point to estimateand the soil line (see details in Biard & Baret (1997)).

Formula	References
Tested in the analysis	
$NDI5 = \frac{\rho_{TM4}-\rho_{TM5}}{\rho_{TM4}+\rho_{TM5}}$	McNairn and Protz (1993)
$NDI7 = \frac{\rho_{TM4}-\rho_{TM7}}{\rho_{TM4}+\rho_{TM7}}$	McNairn and Protz (1993)
$NDTI = \frac{\rho_{TM5}-\rho_{TM7}}{\rho_{TM5}+\rho_{TM7}}$	Van Deventer et al. (1997)
$NDSVI = \frac{\rho_{TM5}-\rho_{TM3}}{\rho_{TM5}+\rho_{TM3}}$	Marsett et al. (2006); Qi et al. (2002)
$Ratio = \frac{\rho_{M7}}{\rho_{M6}}$	Guerschman et al. (2009)
$STI = \frac{\rho_{M6}}{\rho_{M7}}$	Van Deventer et al. (1997)
Not tested in the analysis	
$SACRI = \frac{a(\rho_{TM4}-a\rho_{TM5}-b)}{(\rho_{TM5}+a\rho_{TM4}-ab)}$	Biard et al. (1995)
$MSACRI = C^{ste}\left[\frac{a(\rho_{ETM5}-a\rho_{ETM7}-b)}{(\rho_{ETM7}+a\rho_{ETM5}-ab)}\right]$	Bannari et al. (2000)
$SATVI = \frac{\rho_{TM5}-\rho_{TM3}}{(\rho_{TM5}+\rho_{TM3}+L)}(1+L) - \frac{\rho_{TM7}}{2}$	Marsett et al. (2006)
$DFI = 100\left(1-\frac{\rho_{M7}}{\rho_{M6}}\right)\frac{\rho_{M1}}{\rho_{M2}}$	Cao et al. (2010)
$CRIM = \frac{tan(\delta)}{tan(\zeta)} = \frac{cos(\zeta)}{cos(\delta)} \cdot \sqrt{\frac{1-cos^2(\delta)}{1-cos^2(\zeta)}}$	Biard and Baret (1997)
$CAI = 0,5(\rho_{2031} + \rho_{2211}) - \rho_{2101}$	Daughtry (2001)
$LCA = 100[(\rho_{A6} - \rho_{A5}) + (\rho_{A6} - \rho_{A8})]$	Daughtry et al. (2005)
$SINDRI = 100\left[\frac{\rho_{A6}-\rho_{A7}}{\rho_{A6}+\rho_{A7}}\right]$	Serbin, Hunt, Daughtry, McCarty, and Doraiswamy (2009)